AIMS Mathematics, 7(8): 14249–14269.
DOI: 10.3934/math.2022785
Received: 08 March 2022
Revised: 03 May 2022
Accepted: 06 May 2022
Published: 30 May 2022

http://www.aimspress.com/journal/Math

Research article

Meshfree numerical integration for some challenging multi-term fractional order PDEs

Abdul Samad[1], **Imran Siddique**[2,*] **and Fahd Jarad**[3,4,*]

[1] School of Mathematics, Northwest University Xi'an, 710127, China
[2] Department of Mathematics, University of Management and Technology, Lahore 54770, Pakistan
[3] Department of Mathematics, Cankaya University, Etimesgut, Ankara, Turkey
[4] Department of Medical Research, China Medical University Hospital, China Medical University, Taichung, Taiwan

* **Correspondence:** Email: imransmsrazi@gmail.com, fahd@cankaya.edu.tr; Tel: +925326518721.

Abstract: Fractional partial differential equations (PDEs) have key role in many physical, chemical, biological and economic problems. Different numerical techniques have been adopted to deal the multi-term FPDEs. In this article, the meshfree numerical scheme, Radial basis function (RBF) is discussed for some time-space fractional PDEs. The meshfree RBF method base on the Gaussian function and is used to test the numerical results of the time-space fractional PDE problems. Riesz fractional derivative and Grünwald-Letnikov fractional derivative techniques are used to deal the space fractional derivative terms while the time-fractional derivatives are iterated by Caputo derivative method. The accuracy of the suggested scheme is analyzed by using L_∞-norm. Stability and convergence analysis are also discussed.

Keywords: multi-term fractional derivatives; Caputo and Grünwald-Letnikov derivatives; radial basis function method
Mathematics Subject Classification: 35G31, 35G35, 65D12

1. Introduction

Fractional PDEs have key role in modeling anomalous diffusive process and describe the viscoelastic damping materials. For example in mechanical models, the delivery of oxygen passing through capillaries and anomalous relaxation in magnetic resonance imaging signal magnitude (see [1–4]). However, sometimes it is quite difficult to get the analytical solutions of fractional PDEs (see [5–8]). Therefore numerical methods have popular among the researchers to deal the fractional order PDEs (see [9–13]). Gejji and Bhalekar [17] used the adomain decomposition method,

Jafari and Aminataei [18] used the modified homotopy perturbation method and Liu et al. [19] used some computationally effective numerical methods to deal the fractional order diffusion equations. Further, Bhrawy and Zaky [20] discussed the jacobi tau approximation method, Ren and Sun [21] used the compact difference method for $1D$ and $2D$ multi-term fractional order diffusion equations and Dehghan et al. [22] used the meshless method to solve the fractional PDEs. Finite difference method, interpolating element free galerkin method, spectral element method, galerkin spectral method and finite element method (see [1, 22–26]) are used to discuss the numerical solution of different kind of diffusion equations. Similarly Chen et al. [27, 28] discussed the variable coefficient method and compact dual reciprocity method with the meshless improved singular boundary method. Recently Huang et al. [29] used the alternating direction implicit scheme for the numerical solution of wave diffusion equations.

The multi-term time-space fractional diffusion wave equation (see [29]) is given by

$$\sum_{k=1}^{K} {}_0\mathbb{D}_t^{\alpha_k} v(\chi, t) = \sum_{l=1}^{L} \left(\frac{\partial^{\beta_l}}{\partial |\chi|^{\beta_l}} \right) v(\chi, t) + g(\chi, t), \tag{1.1}$$

with the following initial and boundary conditions

$$\begin{cases} v(\chi, 0) = V(\chi), \quad v_t(\chi, 0) = V_t(\chi), \\ v(a, t) = f_1(t), \quad v(L, t) = f_2(t), \quad t \geq 0, \end{cases} \tag{1.2}$$

where $1 < \beta_l \leq 2$, $D = [a, L]$ is the domain and $\chi = (x)$, $\chi = (x, y)$, $\chi = (x, y, z)$ in $1D, 2D$ and $3D$ respectively. Morever $V(\chi)$, $V_t(\chi)$ and $g(\chi, t)$ are known functions. $v_t(\chi, t)$ is required when $1 < \alpha_k \leq 2$.

To handle different types of PDEs, meshfree methods have got more attraction as compared to the meshgrid methods. Unlike the meshgrid methods, the meshfree methods require a set of uniform scattered points in domain. RBF method is one of the highly attractive meshfree method. The wide application of RBF method can be seen in various practical problems (see [32–37]. RBF method depends on the euclidean distance between two points of the spital domain which is implemented either globally or locally. However, global meshfree RBF method has some problems while dealing high dimensional PDEs. The main problem is that when there is a large number of collocation points, the method tends to ill-conditioning coefficient matrix and the approximated solution becomes unstable. But local RBF method avoids such kind of problems not only in regular domains but also in irregular domains (see [30, 31]). The main feature of local meshfree RBF method is that it is free from ill-conditioning problems which come in large dense matrix systems because these methods use only neighboring collocation points (see [32,38–42]). In such meshfree RBF methods shape parameter plays an important role to bring best possible numerical solution. Multiquadric (MQ), Inverse multiquadric (IMQ) and Gaussian are the most popular functions to implement RBF method. All three functions give good results, but the main issue for these functions is the choice of shape parameter. However in the Gaussian function, if the number of collocation points are increases, the value of shape parameter also increases [43].

Current work base on the applications of meshfree RBF method for the numerical approximation of multi-term fractional order diffusion equations. The fractional space derivatives are dealt by using the definitions of Riesz fractional derivative, Riemann-Liouvelle fractional derivative and Grünwald-Letnikov fractional derivative. The time fractional derivatives are approximated by the Caputo

fractional derivative and finite difference method. The stability and convergence are also discussed in Section 4. The suggested scheme is applied on $1D$, $2D$ and $3D$ multi-term diffusion equations to investigate the numerical tests in Section 5.

2. Preliminary knowledge

The following definitions are useful which are related to fractional derivatives.

Definition 2.1. Let v be defined in the interval $a \leq \chi \leq L$. Then Riesz α-order fractional derivative operator $\mathbb{D}$ is given by [47]

$$\mathbb{D}_{\chi}^{\alpha} v(\chi, t) = \frac{\partial^{\alpha} v(\chi, t)}{\partial |\chi|^{\alpha}} = \mathbb{R}_{\alpha}\Big({}_{a}^{RL}\mathbb{D}_{\chi}^{\alpha} + {}_{\chi}^{RL}\mathbb{D}_{L}^{\alpha}\Big) v(\chi, t), \tag{2.1}$$

where $\mathbb{R}_{\alpha} = -\frac{1}{2\cos(\frac{\pi\alpha}{2})}, \quad \alpha \neq 1 \text{ or } 2.$

Definition 2.2. For $+ve$-integer m, the fractional differential operator $\mathbb{D}$ of order α for Rieman Liouville function is defined by [44, 45]

$${}_{a}^{RL}\mathbb{D}_{\chi}^{\alpha} v(\chi, t) = \frac{1}{\Gamma(m-\alpha)} \frac{d^m}{d\chi^m} \int_{a}^{\chi} v(\psi, t)(\chi - \psi)^{m-\alpha-1} d\psi, \quad m-1 < \alpha \leq m, \tag{2.2}$$

$${}_{\chi}^{RL}\mathbb{D}_{L}^{\alpha} v(\chi, t) = \frac{(-1)^m}{\Gamma(m-\alpha)} \frac{d^m}{d\chi^m} \int_{\chi}^{L} v(\psi, t)(\psi - \chi)^{m-\alpha-1} d\psi,$$

Definition 2.3. The Caputo α-order fractional derivative for $+ve$-integer m is given by [46]

$${}_{0}\mathbb{D}_{t}^{\alpha} v(\chi, t) = \frac{1}{\Gamma(m-\alpha)} \int_{0}^{t} \frac{\partial^m v(\chi, \psi)}{\partial \psi^m} (t - \psi)^{m-\alpha-1} d\psi, \quad m-1 < \alpha \leq m. \tag{2.3}$$

Definition 2.4. The Grünwald-Letnikov α-order fractional derivative for $f(\chi)$ is given by [49]

$${}^{GL}\mathbb{D}_{\chi}^{\alpha} f(\chi) = \lim_{\delta\chi \to 0} \frac{1}{(\delta\chi)^{\alpha}} \sum_{j=0}^{[\frac{\chi-a}{\delta\chi}]} (-1)^j \binom{\alpha}{j} f(\chi - j\delta\chi), \tag{2.4}$$

where $\binom{\alpha}{j} = \frac{\Gamma(\alpha+1)}{\Gamma(j+1)\Gamma(\alpha-j+1)}$.

3. Materials and methods

3.1. Spital discretization via RBF method

In this section the meshfree numerical scheme for Eq (1.1) is discussed. Let $\{\chi_i \in D, i = 1, 2, \cdots, N\}$ be the collocation points in domain $D \subset \mathscr{R}$. Then the approximate solution at s-time level is

$$v(\chi, t_s) = \sum_{j=1}^{N} \xi_j^s \Upsilon(\gamma_j), \tag{3.1}$$

here $\gamma_j = \|\chi - \chi_j\|$, where $\|.\|$ is the euclidean distance between χ and the centers χ_j. For each $\{\chi_i \in D, i = 1, 2, \cdots, N\}$ the respective approximate solution at s-time level is given by.

$$v(\chi_i, t_s) = \sum_{j=1}^{N} \xi_j^s \Upsilon(\gamma_{ij}), \tag{3.2}$$

where $\gamma_{ij} = \|\chi_i - \chi_j\|$, $1 \le i, j \le N$.

Let $A = \Upsilon(\gamma_{ij})$, $v = \{v(\xi_1), v(\xi_2), \cdots, v(\xi_N)\}$ and $\xi = \{\xi_1, \xi_2, \cdots, \xi_N\}^T$, then Eq (3.2) becomes

$$v^s = A\xi^s, \tag{3.3}$$

the coefficient matrix A can further be split into A_d (interior nodes) and A_b (boundry nodes).
Where, $A_d = \{\Upsilon(\gamma_{ij}), 2 \le i \le N-1, 1 \le j \le N\}$ and
$A_b = \{\Upsilon(\gamma_{ij}), i = 1, N, 1 \le j \le N\}$.
Here $\Upsilon(\gamma_{ij}) = \exp(-w\|\chi_i - \chi_j\|^2)$ is called Gaussian radial basis function (GA-RBF), w is the shape parameter. The choice of w is arbitrary. For Gaussian, it is clear that $w = \frac{1}{\sqrt{2}\sigma^2}$, where σ is variance between χ and the centers χ_j (see [43]).

Lemma 3.1.1. If $v(\chi, t) \in L([a, L]\times[0, T])$ and ${}^{RL}\mathbb{D}_{\chi}^{\beta} v(\chi, t) \in C([a, L]\times[0, T])$. Then for $m-1 \le \beta \le m$, where m is positive integer and $i = 1, 2, 3, \cdots, N$. Using Riesz fractional derivative and Riemann-Liouvelle fractional derivative the Grüwald-Letnikov [47] approximation can be obtained

$${}_{a}^{RL}\mathbb{D}_{\chi}^{\beta} v(\chi_i, t) = (\delta\chi)^{-\beta} \sum_{j=0}^{i-1} \varpi_j^{\beta} v(\chi_{i-j}, t) + O(\delta\chi), \tag{3.4}$$

$${}_{\chi}^{RL}\mathbb{D}_{L}^{\beta} v(\chi_i, t) = (\delta\chi)^{-\beta} \sum_{j=0}^{N-i} \varpi_j^{\beta} v(\chi_{i+j}, t) + O(\delta\chi), \tag{3.5}$$

where $\varpi_j^{\beta} = (-1)^j \frac{\Gamma(\beta+1)}{\Gamma(j+1)\Gamma(\beta-j+1)}$ for $j = 0, 1, 2, \cdots$, $\delta\chi = \frac{L-a}{N}$.

Lemma 3.1.2. The coefficients ϖ_j^{β} of Grüwald-Letnikov approximation have the following properties.

(a) $\varpi_1^{\beta} = -\beta$, $\varpi_j^{\beta} \ge 0$ $(j \ne 1)$;

(b) $\sum_{j=0}^{\infty} \varpi_j^{\beta} = 0$;

(c) $\sum_{j=0}^{m} \varpi_j^{\beta} < 0$, where m is any positive integer.

Proof. See [50].

3.2. Time discretization

In this section, the time derivatives of Eq (1.1) will be discretized by Caputo fractional derivative and finite difference method. Let $t_s \in [0, T]$, $\delta t = \frac{T}{S}$, then for $s = 0, 1, 2, \cdots, S$, we have $t_s = s \cdot \delta t$ are the total time discretiztion nodes. From Eq (2.3), for $m = 1$ or 2, let us rewrite the Caputo fractional derivative of order α as

$${}_0\mathbb{D}_t^{\alpha} v(\chi, t) = \begin{cases} \frac{1}{\Gamma(1-\alpha)} \int_0^t \frac{\partial u(z,\psi)}{\partial \psi} (t-\psi)^{-\alpha} d\psi, & 0 < \alpha < 1, \\ \frac{\partial v(\chi,t)}{\partial t}, & \alpha = 1, \\ \frac{1}{\Gamma(2-\alpha)} \int_0^t \frac{\partial^2 v(\chi,\psi)}{\partial \psi^2} (t-\psi)^{1-\alpha} d\psi, & 1 < \alpha < 2, \\ \frac{\partial^2 v(\chi,t)}{\partial t^2}, & \alpha = 2. \end{cases} \tag{3.6}$$

Case I. When $0 < \alpha \leq 1$, using the finite difference method to approximate the time fractional term of Eq (3.6), we have

$$
\begin{aligned}
{}_0\mathbb{D}_t^{\alpha} v(\chi, t_{s+1}) &= \frac{1}{\Gamma(1-\alpha)} \int_0^{t_{s+1}} \frac{\partial v(\chi,\psi)}{\partial \psi} (t_{s+1}-\psi)^{-\alpha} d\psi \\
&= \frac{1}{\Gamma(1-\alpha)} \sum_{q=0}^{s} \int_{t_q}^{t_{q+1}} \frac{\partial v(\chi,t)}{\partial \psi} \frac{d\psi}{(t_{q+1}-\psi)^{\alpha}} \\
&= \frac{1}{\Gamma(1-\alpha)} \sum_{q=0}^{s} \frac{v(\chi,t_{q+1}) - v(\chi,t_q)}{\delta t} \int_{t_q}^{t_{q+1}} \frac{d\psi}{(t_{q+1}-\psi)^{\alpha}} + \rho_{\delta t}^{s+1} \\
&= \frac{1}{\Gamma(1-\alpha)} \sum_{q=0}^{s} \frac{v(\chi,t_{q+1}) - v(\chi,t_q)}{\delta t} \int_{t_{s-q}}^{t_{s+1-q}} \frac{d\varrho}{\varrho^{\alpha}} + \rho_{\delta t}^{s+1} \\
&= \frac{1}{\Gamma(2-\alpha)} \sum_{q=0}^{s} \frac{v(\chi,t_{s-q+1}) - v(\chi,t_{s-q})}{(\delta t)^{\alpha}} [(q+1)^{1-\alpha} - (q)^{1-\alpha}] + \rho_{\delta t}^{s+1}.
\end{aligned}
$$

Thus the time discretization for $0 < \alpha < 1$, becomes

$$
{}_0\mathbb{D}_t^{\alpha} v(\chi, t_{s+1}) = \begin{cases} r_\alpha (v^{s+1} - v^s) + r_\alpha \sum_{q=1}^{s} \delta_q^{\alpha} (v^{s+1-q} - v^{s-q}) + \rho_{\delta t}^{s+1}, & s \geq 1 \\ r_\alpha (v^1 - v^0), & s = 0, \end{cases} \tag{3.7}
$$

where $r_\alpha = \frac{(\delta t)^{-\alpha}}{\Gamma(2-\alpha)}$, $\delta_q^{\alpha} = (q+1)^{1-\alpha} - (q)^{1-\alpha}$, $\varrho = t_{s+1} - \psi$, for $q = 0, 1, \cdots, s$ and $\rho_{\delta t}^{s+1}$ is the truncation error.

Case II. When $1 < \alpha \leq 2$, the time discretization is

$$
{}_0\mathbb{D}_t^{\alpha} v(\chi, t_{s+1}) = \frac{1}{\Gamma(2-\alpha)} \sum_{q=0}^{s} \int_{t_q}^{t_{q+1}} \frac{\partial^2 v(\chi,\psi)}{\partial \psi^2} (t_{s+1}-\psi)^{1-\alpha} d\psi. \tag{3.8}
$$

Now

$$
\frac{\partial^2 v(\chi, t_{s+1})}{\partial t^2} = \frac{v^{s+1} - 2v^s + v^{s-1}}{\delta t^2} + O(\delta t)^2, \tag{3.9}
$$

insert in Eq (3.8) and using the finite difference method, we get

$$
{}_0\mathbb{D}_t^{\alpha} v(\chi, t_{s+1}) = r_\alpha (v^{s+1} - 2v^s + v^{s-1}) + r_\alpha \sum_{q=1}^{s} \delta_q^{\alpha} (v^{s-q+1} - 2v^{s-q} + v^{s-q-1}) + \rho_{(\delta t)^2}^{s+1}, \qquad s \geq 0, \tag{3.10}
$$

where $r_\alpha = \frac{(\delta t)^{-\alpha}}{\Gamma(3-\alpha)}$ and $\delta_q^{\alpha} = (q+1)^{2-\alpha} - q^{2-\alpha}$ for $q = 0, 1, 2, \cdots, s$.

Since for $s = 0$ and $q = s$ there exists an unknown $v(\chi, t_{-1})$. To eliminate the unknown term, using $v_t(\chi, t_0)$ by central difference method, we have

$$
\begin{aligned}
v_t(\chi, t_0) &= \frac{v(\chi, t_1) - v(\chi, t_{-1})}{2\delta t}, \\
v(\chi, t_{-1}) &= v(\chi, t_1) - 2\delta t v_t(\chi, t_0).
\end{aligned}
$$

Thus for $1 < \alpha < 2$ the time discretization becomes

$$ {}_0\mathbb{D}_t^{\alpha} v(\chi, t_{s+1}) = \begin{cases} r_\alpha(v^{s+1} - 2v^s + v^{s-1}) + r_\alpha \sum_{q=1}^{s-1} \delta_q^\alpha (v^{s-q+1} - 2v^{s-q} + v^{s-q-1}) \\ \quad +2r_\alpha \delta_s^\alpha (v^1 - v^0 - \delta t v_t^0), \qquad s \geq 1 \\ 2r_\alpha(v^1 - v^0 - \delta t v_t^0), \qquad\qquad s = 0. \end{cases} \tag{3.11} $$

Lemma 3.2.1. If $0 < \alpha < 1$, $\phi(t)$ is a function defined in $C^2[0, T]$, then for $0 \leq s \leq N$, the following properties are true

$$ \int_0^{t_{s+1}} \phi'(\psi)(t_{s+1} - \psi)^{-\alpha} d\psi = \sum_{q=0}^{s} \frac{\phi(t_{q+1}) - \phi(t_q)}{\delta t} \int_{t_q}^{t_{q+1}} (t_{s+1} - \psi)^{-\alpha} d\psi + \rho_{\delta t}^{s+1}, $$

and

$$ |\rho_{\delta t}^{s+1}| \leq \left(\frac{1}{2} + \frac{1}{2(1-\alpha)}\right) \delta t^{2-\alpha} \max_{0 \leq t \leq t_{s+1}} |\phi''(t)|. $$

Proof. See [48].

Lemma 3.2.2. Let $0 < \alpha < 1$, $r_\alpha = \frac{1}{\delta t \Gamma(1-\alpha)}$ and $\delta_q^\alpha = \frac{\delta t^{1-\alpha}}{1-\alpha}[(q+1)^{1-\alpha} - q^{1-\alpha}]$, then

$$ \left| \frac{1}{\Gamma(1-\alpha)} \int_0^{t_{s+1}} \frac{\phi'(\psi)}{(t_{s+1} - \psi)^{\alpha}} d\psi - r_\alpha \left[\delta_0^\alpha \phi(t_{s+1}) - \sum_{q=1}^{s} (\delta_{s-q}^\alpha - \delta_{s-q+1}^\alpha) \phi(t_q) - \delta_s^\alpha \phi(0) \right] \right| $$

$$ \leq \frac{1}{2\Gamma(1-\alpha)} \left(\frac{1}{(1-\alpha)} + 1 \right) \delta t^{2-\alpha} \max_{0 \leq t \leq t_{s+1}} |\phi''(t)|. $$

Proof. Follows from Lemma 3.2.1.

Lemma 3.2.3. Let $\delta_q^\alpha = \frac{\delta t^{1-\alpha}}{(1-\alpha)}\left[(q+1)^{1-\alpha} - (q)^{1-\alpha}\right]$, where $q = 1, 2, ...$, and $0 < \alpha < 1$, then $\delta_0^\alpha > \delta_1^\alpha > \delta_2^\alpha > .....\delta_q^\alpha \to 0$ as $q \to \infty$.

Proof. For proof (see [48]).

Lemma 3.2.4. If $1 < \alpha < 2$, $\phi(t)$ is a function defined in $C^2[0, T]$, then for $0 \leq s \leq N$, the following properties are true

$$ \int_0^{t_{s+1}} \phi'(\psi)(t_{s+1} - \psi)^{1-\alpha} d\psi = \sum_{q=0}^{s} \frac{\phi(t_{q+1}) - \phi(t_q)}{\delta t} \int_{t_q}^{t_{q+1}} (t_{s+1} - \psi)^{1-\alpha} d\psi + \rho_{\delta t}^{s+1}, $$

and

$$ |\rho_{\delta t}^{s+1}| \leq \left(\frac{1}{2} + \frac{1}{2(1-\alpha)}\right) \delta t^{3-\alpha} \max_{0 \leq t \leq t_{s+1}} |\phi''(t)|. $$

Proof. See [48].

Lemma 3.2.5. Let $1 < \alpha < 2$, $r_\alpha = \frac{1}{\delta t \Gamma(2-\alpha)}$ and $\delta_q^\alpha = \frac{\delta t^{2-\alpha}}{2-\alpha}[(q+1)^{2-\alpha} - q^{2-\alpha}]$, then

$$ \left| \frac{1}{\Gamma(2-\alpha)} \int_0^{t_{s+1}} \frac{\phi'(\psi)}{(t_{s+1} - \psi)^{\alpha-1}} d\psi - r_\alpha \left[\delta_0^\alpha \phi(t_{s+1}) - \sum_{q=1}^{s} (\delta_{s-q}^\alpha - \delta_{s-q+1}^\alpha) \phi(t_q) - \delta_s^\alpha \phi(0) \right] \right| $$

$$\leq \frac{1}{2\Gamma(2-\alpha)}\Big(\frac{1}{(2-\alpha)}+1\Big)\delta t^{3-\alpha}\max_{0\leq t\leq t_{s+1}}|\phi''(t)|.$$

Proof. Follows from Lemma 3.2.5.

Lemma 3.2.6. Let $\delta_q^\alpha = \frac{\delta t^{2-\alpha}}{(2-\alpha)}\Big[(q+1)^{2-\alpha}-(q)^{2-\alpha}\Big]$, where $q = 1, 2, ...$, and $1 < \alpha < 2$, then $\delta_0^\alpha > \delta_1^\alpha > \delta_2^\alpha > .....\delta_q^\alpha \to 0$ as $q \to \infty$

Proof. For proof (see [48]).

3.3. Numerical scheme

In this part the numerical scheme for Eq (1.1) will be computed by using θ-weighted method. For this let $\mathscr{L}^\beta v = \frac{\partial^\beta v}{\partial|\chi|^\beta}$, $g(\chi,t) = \mathcal{g}$, then Eq (1.1) can be written as

$$\sum_{k=1}^{K} {}_0\mathbb{D}_t^{\alpha_k} v = \sum_{l=1}^{L}\mathscr{L}^{\beta_l} v + \mathcal{g}. \tag{3.12}$$

Now at time s and $s+1$ level, applying θ-weighted method to Eq (3.12), where $0 \leq \theta \leq 1$, we get

$$\sum_{k=1}^{K} {}_0\mathbb{D}_t^{\alpha_k} v^{s+1} = \theta\sum_{l=1}^{L}\mathscr{L}^{\beta_l} v^{s+1} + (1-\theta)\sum_{l=1}^{L}\mathscr{L}^{\beta_l} v^s + \mathcal{g}^{s+1}, \qquad s \geq 0, \tag{3.13}$$

Case I. For $0 < \alpha_k \leq 1$ using Eq (3.11) and for space derivative using Eqs (2.1), (3.4) and (3.5) we get

$$\begin{aligned}\sum_{k=1}^{K}\Big(r_{\alpha_k}(v^{s+1}-v^s) + r_{\alpha_k}\sum_{q=1}^{s}\delta_q^{\alpha_k}(v^{s+1-q}-v^{s-q})\Big) =& \theta\sum_{l=1}^{L}\frac{(\delta\chi)^{-\beta_l}}{-2\cos(\frac{\pi\beta_l}{2})}\Big(G_{\beta_l}+G_{\beta_l}^T\Big)v^{s+1}\\ &+(1-\theta)\sum_{l=1}^{L}\frac{(\delta\chi)^{-\beta_l}}{-2\cos(\frac{\pi\beta_l}{2})}\Big(G_{\beta_l}+G_{\beta_l}^T\Big)v^s + \mathcal{g}^{s+1},\end{aligned} \tag{3.14}$$

where $G_{\beta_l} = \begin{bmatrix} \varpi_0^{\beta_l} & 0 & \cdots & 0\\ \varpi_1^{\beta_l} & \varpi_0^{\beta_l} & \cdots & 0\\ \vdots & \vdots & \ddots & 0\\ \varpi_{N-1}^{\beta_l} & \varpi_{N-2}^{\beta_l} & \cdots & \varpi_0^{\beta_l}\end{bmatrix}$, and $\varpi_j^{\beta_l} = (-1)^j\frac{\Gamma(\beta_l+1)}{\Gamma(j+1)\Gamma(\beta_l-j+1)}$, for $j = 0, 1, 2, \cdots$.

Thus Eq (3.14) can be written as

$$\begin{aligned}\sum_{k=1}^{K} r_{\alpha_k} v^{s+1} - \theta\sum_{l=1}^{L}\frac{(\delta\chi)^{-\beta_l}}{-2\cos(\frac{\pi\beta_l}{2})}\Big(G_{\beta_l}+G_{\beta_l}^T\Big)v^{s+1} =& \sum_{k=1}^{K} r_{\alpha_k} v^s + (1-\theta)\sum_{l=1}^{L}\frac{(\delta\chi)^{-\beta_l}}{-2\cos(\frac{\pi\beta_l}{2})}\Big(G_{\beta_l}+G_{\beta_l}^T\Big)v^s\\ &-\sum_{k=1}^{K} r_{\alpha_k}\sum_{q=1}^{s}\delta_q^{\alpha_k}(v^{s+1-q}-v^{s-q}) + \mathcal{g}^{s+1},\end{aligned} \tag{3.15}$$

Insert Eq (3.3) into Eq (3.15), we get

$$\sum_{k=1}^{K} r_{\alpha_k} A\xi^{s+1} - \theta \sum_{l=1}^{L} \frac{(\delta\chi)^{-\beta_l}}{-2\cos(\frac{\pi\beta_l}{2})}\Big(G_{\beta_l} + G_{\beta_l}^T\Big)A\xi^{s+1} = \sum_{k=1}^{K} r_{\alpha_k} A\xi^{s} + (1-\theta)\times$$
$$\sum_{l=1}^{L} \frac{(\delta\chi)^{-\beta_l}}{-2\cos(\frac{\pi\beta_l}{2})}\Big(G_{\beta_l} + G_{\beta_l}^T\Big)A\xi^{s} - \sum_{k=1}^{K} r_{\alpha_k} \sum_{q=1}^{s} \delta_q^{\alpha_k}(v^{s+1-q} - v^{s-q}) + \mathcal{g}^{s+1}. \tag{3.16}$$

Let

$$\mathscr{M} = \sum_{k=1}^{K} r_{\alpha_k} A - \theta \sum_{l=1}^{L} \frac{(\delta\chi)^{-\beta_l}}{-2\cos(\frac{\pi\beta_l}{2})}\Big(G_{\beta_l} + G_{\beta_l}^T\Big)A,$$

$$\mathscr{N} = \sum_{k=1}^{K} r_{\alpha_k} A + (1-\theta) \sum_{l=1}^{L} \frac{(\delta\chi)^{-\beta_l}}{-2\cos(\frac{\pi\beta_l}{2})}\Big(G_{\beta_l} + G_{\beta_l}^T\Big)A,$$

$$\mathscr{F}_1^{s+1} = \sum_{k=1}^{K} r_{\alpha_k} \sum_{q=1}^{s} \delta_q^{\alpha_k}(v^{s+1-q} - v^{s-q}) + \mathcal{g}^{s+1},$$

$$\mathscr{F}_2^{s+1} = [V^{s+1}(a), 0, \cdots, 0, V^{s+1}(L)]^T$$

and $\mathscr{F}^{s+1} = \mathscr{F}_2^{s+1} - \mathscr{F}_1^{s+1}$, then Eq (3.16) can be written as

$$\mathscr{M}\xi^{s+1} = \mathscr{N}\xi^{s} + \mathscr{F}^{s+1}, \tag{3.17}$$

Thus the required numerical scheme for $0 < \alpha_k \le 1$ and $1 < \beta_l \le 2$, is obtained

$$v^{s+1} = A\mathscr{M}^{-1}\mathscr{N}A^{-1}v^{s} + A\mathscr{M}^{-1}\mathscr{F}^{s+1}, \quad s \ge 0. \tag{3.18}$$

Case II. When $1 < \alpha_k \le 2$, use Eq (3.11) into Eq (3.14), we have

$$\sum_{k=1}^{K} r_{\alpha_k}(v^{s+1} - 2v^{s} + v^{s-1}) + \sum_{k=1}^{K} r_{\alpha_k} \sum_{q=1}^{s-1} \delta_q^{\alpha_k}(v^{s-q+1} - 2v^{s-q} + v^{s-q-1}) + \sum_{k=1}^{K} 2r_{\alpha_k}\delta_s^{\alpha}(v^1 - v^0 - \delta t v_t^0)$$
$$= \theta \sum_{l=1}^{L} \frac{(\delta\chi)^{-\beta_l}}{-2\cos(\frac{\pi\beta_l}{2})}\Big(G_{\beta_l} + G_{\beta_l}^T\Big)v^{s+1} + (1-\theta) \sum_{l=1}^{L} \frac{(\delta\chi)^{-\beta_l}}{-2\cos(\frac{\pi\beta_l}{2})}\Big(G_{\beta_l} + G_{\beta_l}^T\Big)v^{s} + \mathcal{g}^{s+1}. \tag{3.19}$$

For $s = 0$, Eq (3.19) becomes

$$\sum_{k=1}^{K} 2r_{\alpha_k}(v^1 - v^0 - \delta t v_t^0) - \theta \sum_{l=1}^{L} \frac{(\delta\chi)^{-\beta_l}}{-2\cos(\frac{\pi\beta_l}{2})}\Big(G_{\beta_l} + G_{\beta_l}^T\Big)v^1 = (1-\theta) \sum_{l=1}^{L} \frac{(\delta\chi)^{-\beta_l}}{-2\cos(\frac{\pi\beta_l}{2})}\Big(G_{\beta_l} + G_{\beta_l}^T\Big)v^0 + \mathcal{g}^1, \tag{3.20}$$

here

$$\mathscr{M}_0 = \sum_{k=1}^{K} 2r_{\alpha_k} A - \theta \sum_{l=1}^{L} \frac{(\delta\chi)^{-\beta_l}}{-2\cos(\frac{\pi\beta_l}{2})}\Big(G_{\beta_l} + G_{\beta_l}^T\Big)A,$$

$$\mathscr{N}_0 = \sum_{k=1}^{K} 2r_{\alpha_k} A + (1-\theta) \sum_{l=1}^{L} \frac{(\delta\chi)^{-\beta_l}}{-2\cos(\frac{\pi\beta_l}{2})}\Big(G_{\beta_l} + G_{\beta_l}^T\Big)A,$$

$$\mathscr{F}_2^1 = [V^1(a), 0, \cdots, 0, V^1(L)]^T,$$
$$\mathscr{F}^1 = \mathscr{F}_2^1 - 2\delta t v_t^0.$$

Thus for $s = 0$ the numerical scheme is

$$v^1 = A\mathscr{M}_0\mathscr{N}_0 A^{-1}v^0 + \mathscr{F}^1. \tag{3.21}$$

For $s \geq 1$, Eq (3.19) implies

$$\sum_{k=1}^{K} r_{\alpha_k} A\xi^{s+1} - \theta \sum_{l=1}^{L} \frac{(\delta\chi)^{-\beta_l}}{-2\cos\left(\frac{\pi\beta_l}{2}\right)}\left(G_{\beta_l} + G_{\beta_l}^T\right)A\xi^{s+1} = \sum_{k=1}^{K} 2r_{\alpha_k} A\xi^s + (1-\theta)\sum_{l=1}^{L} \frac{(\delta\chi)^{-\beta_l}}{-2\cos\left(\frac{\pi\beta_l}{2}\right)}\left(G_{\beta_l} + G_{\beta_l}^T\right)A\xi^s$$
$$- \sum_{k=1}^{K} r_{\alpha_k} \sum_{q=1}^{s-1} \delta_q^{\alpha_k}(v^{s-q+1} - 2v^{s-q} + v^{s-q-1}) - \sum_{k=1}^{K} 2r_{\alpha_k}\delta_s^{\alpha}(v^1 - v^0 - \delta t v_t^0) + \mathscr{g}^{s+1}, \tag{3.22}$$

again let

$$\mathscr{M} = \sum_{k=1}^{K} r_{\alpha_k} A - \theta \sum_{l=1}^{L} \frac{(\delta\chi)^{-\beta_l}}{-2\cos\left(\frac{\pi\beta_l}{2}\right)}\left(G_{\beta_l} + G_{\beta_l}^T\right)A,$$

$$\mathscr{N} = \sum_{k=1}^{K} 2r_{\alpha_k} A + (1-\theta)\sum_{l=1}^{L} \frac{(\delta\chi)^{-\beta_l}}{-2\cos\left(\frac{\pi\beta_l}{2}\right)}\left(G_{\beta_l} + G_{\beta_l}^T\right)A,$$

$$\mathscr{P} = \sum_{k=1}^{K} r_{\alpha_k} I,$$

$$\mathscr{F}_1^{s+1} = \sum_{k=1}^{K}\left(r_{\alpha_k}\sum_{q=1}^{s-1}\delta_q^{\alpha_k}(v^{s-q+1} - 2v^{s-q} + v^{s-q-1}) + 2r_{\alpha_k}\delta_s^{\alpha_k}(v^1 - v^0 - \delta t v_t^0)\right),$$

$$\mathscr{F}_2^{s+1} = [V^{s+1}(a), 0, \cdots, 0, V^{s+1}(L)]^T$$

and

$$\mathscr{F}^{s+1} = \mathscr{F}_2^{s+1} - \mathscr{F}_1^{s+1} + \mathscr{g}^{s+1}.$$

Thus for $1 < \alpha_k \leq 2$ and $s \geq 1$ the numerical scheme for Eq (3.19) is

$$v^{s+1} = A\mathscr{M}^{-1}\mathscr{N}A^{-1}v^s + A\mathscr{M}^{-1}\mathscr{P}v^{s-1} + A\mathscr{M}^{-1}\mathscr{F}^{s+1}. \tag{3.23}$$

4. Stability and convergence analysis

In this section, the stability and convergence analysis for Eqs (3.18) and (3.23) are discussed. Let υ^s and v^s be the respective exact and numerical solutions of Eq (1.1) at time s level. The amplification matrix $\mathbb{J} = A\mathscr{M}^{-1}\mathscr{N}A^{-1}$ depends on $\hbar = \frac{(\delta t)^{\alpha}}{(\delta\chi)^{\beta}}$, which is a constant number. $[\alpha, \beta] = \max[\alpha_k, \beta_l]$ are the fractional orders of time and space derivatives and δt , $\delta\chi$ are the time step and space step respectively. In order to check the stability and convergence, we need to know some important results (see [43] for

proof see [32]) which are given by

Theorem 4.1.

$$\left|\mathbb{D}^{\alpha}g(\chi)-\mathbb{D}^{\alpha}P_{g}(\chi)\right|\leq\mathscr{C}\delta\chi_{x,\Gamma}^{k-|\alpha|}\sqrt{\mathscr{C}_{\Theta}(\chi)}\left|g_{\aleph_{\phi}}(\Gamma)\right|,$$

provided that $(\delta\chi)_{x,\Gamma}\leq(\delta\chi)_{0}$, where

$$\mathscr{C}_{\Theta}(\chi)=\max_{\substack{\alpha_1,\alpha_2\in\mathbb{N}_0^r w,\chi\in\Gamma\cap B(\chi,c_2\delta\chi_x,\Gamma)\\ |\alpha_1|+|\alpha_2|=2k}}\max\left|\mathbb{D}_1^{\alpha_1}\mathbb{D}_2^{\alpha_2}\Theta(w,\chi)\right|.$$

Theorem 4.2. Let an open and bounded set $\Lambda\subseteq\mathscr{R}^{s}$ that satisfies the condition of interior cone and let $\Theta\in\mathbb{C}^{2k}(\Lambda\times\Lambda)$ is symmetric and strictly conditionally positive definite of order n on $\mathscr{R}^{s}$. Assign the interpolant to $g\in\aleph_{\phi}(\Lambda)$ on the $(n-1)$ unisolvent set x by P_g. Fix $\alpha\in\mathbb{N}_0^r$, taking $|\alpha|\leq k$. Then there exist positive constants $\delta\chi_0$ and C (independent of χ, g, Θ) such that

$$\left|\mathbb{D}^{\alpha}g(\chi)-\mathbb{D}^{\alpha}P_{g}(\chi)\right|\leq C_{k}(\delta\chi)^{k-|\alpha|}\left|v_{\aleph_{\phi}(\Lambda)}\right|,$$

where $\aleph_{\phi}(\Lambda)$ represents the native space of RBF and also $g\in\aleph_{\phi}(\Lambda)$. Since Gaussian is infinitely smooth function so therefore above theorem is applicable and yield high algebraic convergence rates. Hence the conclusion is that for all $k\in\mathbb{N}$ and $|\alpha|\leq k$, we have

$$\left|\mathbb{D}^{\alpha}\upsilon(\chi)-\mathbb{D}^{\alpha}v(\chi)\right|\leq C_{k}(\delta\chi)^{k-|\alpha|}\left|v_{\aleph_{\phi}(\Lambda)}\right|,$$

where v and υ are the respective numerical and exact solutions. Assume that Eq (3.18) of space order β_l where $1<\beta_l\leq 2$ is accurate, then

$$v^{s+1}=\mathbb{J}u^{s}+A\mathscr{M}^{-1}\mathscr{F}^{s+1}+o\Big((\delta t)^{2-\alpha}+(\delta\chi)^{\beta}\Big),\quad \delta t,\delta\chi\longrightarrow 0. \tag{4.1}$$

Let us define the residual by $e^{s}=\upsilon^{s}-u^{s}$, then

$$e^{s+1}=\mathbb{J}e^{s}+o\Big((\delta t)^{2-\alpha}+(\delta\chi)^{\beta}\Big),\quad \delta t,\delta\chi\longrightarrow 0. \tag{4.2}$$

Using Lax-Richtmyer definition of stability, the numerical scheme Eq (3.18) is stable if

$$\|\mathbb{J}\|\leq 1, \tag{4.3}$$

$\|\mathbb{J}\|=\rho(\mathbb{J})$, when $\mathbb{J}$ is normal otherwise $\rho(\mathbb{J})\leq\|\mathbb{J}\|$ is always satisfied. Let us suppose that $\delta\chi$ is small such that the solution and initial condition of the source problem must be sufficiently smooth then we necessarily have $\delta t\longrightarrow 0$ such that it keeps the value of $\hbar=\frac{\delta t}{(\delta\chi)^{\beta_l}}$ constant. Therefore there exist $\wp$ such that

$$\|e^{s+1}\|\leq\|\mathbb{J}\|\|e^{s}\|+\wp\Big((\delta t)^{2-\alpha}+(\delta\chi)^{\beta}\Big),\quad s\geq 0. \tag{4.4}$$

Since e^{s} obeys the initial and boundary conditions, so $e^{(0)}=0$. Hence it follows from mathematical induction

$$\|e^{s+1}\|\leq\Big(1+\|\mathbb{J}\|+\|\mathbb{J}\|^{2}+\cdots+\|\mathbb{J}\|^{s-1}\Big)\wp\Big((\delta t)^{2-\alpha}+(\delta\chi)^{\beta}\Big),\quad s\geq 0. \tag{4.5}$$

Using Eq (4.3), we have

$$\|e^{s+1}\|\leq s\wp\Big((\delta t)^{2-\alpha}+(\delta\chi)^{\beta}\Big). \tag{4.6}$$

Hence the numerical scheme in Eq (3.18) is convergent. Similarly the convergence for the numerical scheme in Eq (3.23) can be shown

$$\|e^{s+1}\|\leq s\wp\Big((\delta t)^{3-\alpha}+(\delta\chi)^{\beta}\Big). \tag{4.7}$$

5. Numerical results and siscussion

In this part the numerical results of multi-term diffusion-wave equations are discussed. The accuracy of the scheme at time level s is measured by

$$L_\infty = \max_{1\le j\le N} \|\upsilon_j^s - v_j^s\|,$$

where υ and v are the exact and numerical solutions respectively. The following equations are used to test the convergence rate w.r.t space and time

$$S\,pital\ order = \frac{\log_{10}(\|\upsilon - v_{\delta\chi_i}\|/\|\upsilon - v_{\delta\chi_{i+1}}\|)}{\log_{10}(\delta\chi_i/\delta\chi_{i+1})},$$

$$Time\ order = \frac{\log_{10}(\|\upsilon - v_{\delta t_i}\|/\|\upsilon - v_{\delta t_{i+1}}\|)}{\log_{10}(\delta t_i/\delta t_{i+1})}.$$

Test Problem 1. Consider the following one-dimensional, three terms fractional PDE

$$\left({}_0\mathbb{D}_t^{\alpha_1} + {}_0\mathbb{D}_t^{\alpha_2} + {}_0\mathbb{D}_t^{\alpha_3}\right)v(\chi,t) = \sum_{l=1}^{3} \frac{\partial^{\beta_l}}{\partial|\chi|^{\beta_l}} v(\chi,t) + g(\chi,t), \quad t \ge 0, \quad -2 \le \chi \le 2,$$

with the initial and boundary conditions $v(\chi,0) = 0, \quad v(-2,t) = e^{-2}\cdot t, \quad v(2,t) = e^2\cdot t,$
where $0 < \alpha_1, \alpha_2, \alpha_3 \le 1$ and $1 < \beta_1, \beta_2, \beta_3 \le 2$.
The exact solution is $\upsilon(\chi,t) = e^{\chi}t$ and $g(\chi,t) = \sum_{k=1}^{3}\left(\frac{t^{1-\alpha_k}}{\Gamma(2-\alpha_k)}e^{\chi} + \frac{3te^{\chi}}{2\cos\frac{\pi\beta_k}{2}}\right)$.
The calculations in Table 1 is computed by taking $\alpha_1 = 0.2$, $\alpha_2 = 0.3$, $\alpha_3 = 0.5$, $\beta_1 = 1.5$, $\beta_2 = 1.6$ and $\beta_3 = 1.8$ respectively, and the graphical results are shown in Figure 1.

Table 1. Numerical results of Problem 1.

		L_∞-norm			Convergence					
		$\delta t = 0.1$	$\delta t = 0.01$	$\delta t = 0.001$	$\delta\chi_i$	L_∞	order	δt_i	L_∞	order
$\theta = 0.5$	$N = 50$	$3.1531e^{-3}$	$2.7480e^{-3}$	$2.3322e^{-3}$	0.08	$2.3322e^{-3}$	—-	0.1	$9.2076e^{-5}$	—-
	$N = 100$	$2.0111e^{-3}$	$1.4786e^{-3}$	$9.9889e^{-4}$	0.04	$9.9889e^{-4}$	−0.6559	0.05	$7.8025e^{-5}$	0.2389
	$N = 500$	$6.1112e^{-4}$	$5.8443e^{-4}$	$5.1733e^{-4}$	0.008	$5.1733e^{-4}$	0.4088	0.01	$1.7136e^{-5}$	0.9418
	$N = 1000$	$1.5128e^{-4}$	$1.2021e^{-4}$	$1.0064e^{-4}$	0.004	$1.0064e^{-4}$	2.3619	0.005	$1.5307e^{-5}$	0.1628
	$N = 2000$	$9.2076e^{-5}$	$1.7136e^{-5}$	$1.4994e^{-5}$	0.002	$1.4994e^{-5}$	0.8675	0.001	$1.4994e^{-5}$	0.0128
$\theta = 1$	$N = 50$	$2.2231e^{-3}$	$1.4774e^{-3}$	$1.2021e^{-3}$	0.08	$1.2021e^{-3}$	—-	0.1	$7.8162e^{-5}$	—-
	$N = 100$	$1.8143e^{-3}$	$1.2663e^{-3}$	$9.6978e^{-4}$	0.04	$9.6978e^{-4}$	−1.5694	0.05	$5.1026e^{-5}$	0.6152
	$N = 500$	$5.9321e^{-4}$	$4.9506e^{-4}$	$5.7903e^{-4}$	0.008	$5.7903e^{-4}$	0.3204	0.01	$1.0061e^{-5}$	1.0088
	$N = 1000$	$1.3412e^{-4}$	$1.0211e^{-4}$	$9.9978e^{-5}$	0.004	$9.9978e^{-5}$	0.6547	0.005	$9.5492e^{-6}$	−1.8039
	$N = 2000$	$7.8162e^{-5}$	$1.0061e^{-5}$	$7.8898e^{-6}$	0.002	$7.8898e^{-6}$	1.7843	0.001	$7.8898e^{-6}$	0.1186

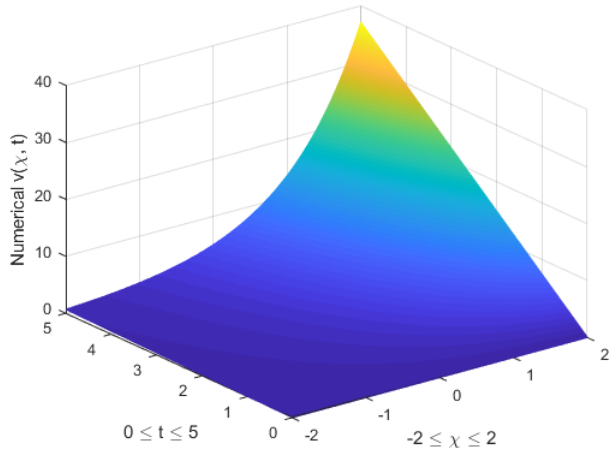

(a) Numerical $v(\chi, t)$ graph

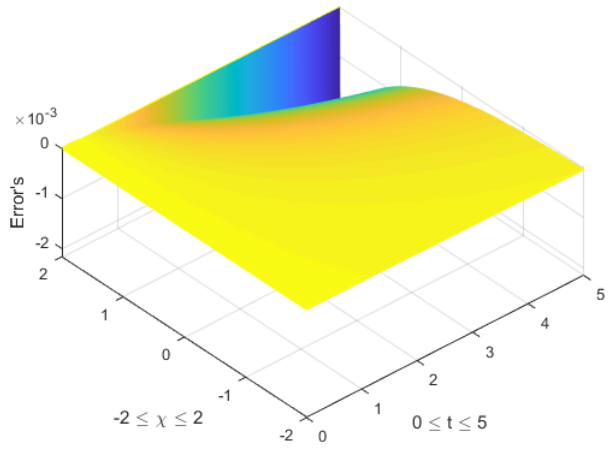

(b) Error graph

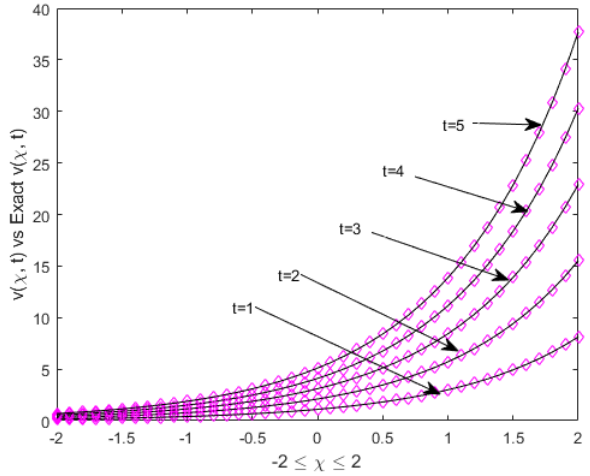

(c) Numerical $v(\chi, t)$

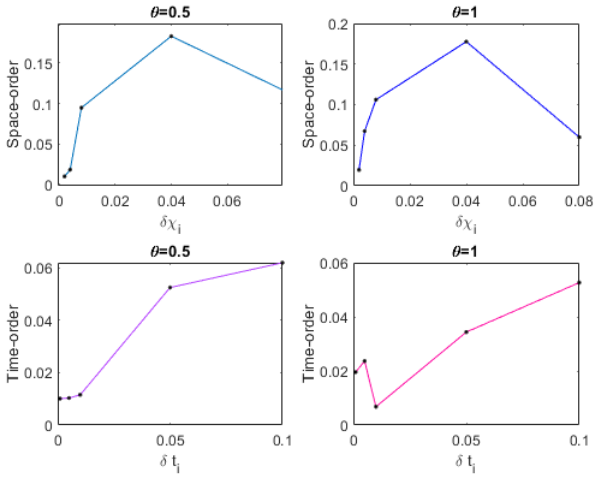

(d) Time and Space convergence graph

Figure 1. Numerical results of Problem 1.

Test Problem 2. Consider two-dimensional, two term fractional PDE

$$\left({}_0\mathbb{D}_t^{\alpha_1} + {}_0\mathbb{D}_t^{\alpha_2}\right)v(\chi, t) = \sum_{l=1}^{2} \frac{\partial^{\beta_l}}{\partial|\chi|^{\beta_l}} v(\chi, t) + g(\chi, t), \quad 0 \le \chi \le 1, \quad t \ge 0,$$

here $1 < \alpha_k \le 2$, $1 < \beta_k \le 2$,

$\chi = (x, y)$, Domain $D = [0, 1]^2$ and

$\frac{\partial^\beta}{\partial|\chi|^\beta} = \left(\frac{\partial^\beta}{\partial|x|^\beta} + \frac{\partial^\beta}{\partial|y|^\beta}\right)$ with the following initial and boundary conditions;

$v\chi, 0) = 0, \quad v_t(\chi, 0) = 0,$

$v(0, t) = 0, \quad v(1, t) = 0.$

$$g(x, y, t) = \Gamma(2 + \alpha_1)t(x^2 - x^4)(y^2 - y^4) + \frac{\Gamma(2 + \alpha_1)}{\Gamma(2 - \alpha_2 + \alpha_1)} t^{1-\alpha_2+\alpha_1}(x^2 - x^4)(y^2 - y^4)$$
$$+ t^{1+\alpha_1}[Q(x, y, \beta_k) + Q(y, x, \beta_k)],$$

where

$$Q(x,y,\beta_k) = \frac{x^2 - x^4}{\cos\left(\frac{\pi\beta_k}{2}\right)\Gamma(5-\beta_k)}\Big(12(y^{4-\beta_k} + (1-y)^{4-\beta_k} - 6(4-\beta_k)\times$$
$$(y^{3-\beta_k} + (1-y)^{3-\beta_k}) + (3-\beta_k)(4-\beta_k)(y^{2-\beta} + (1-y)^{2-\beta})\Big),$$

and

$$Q(y,x,\beta_k) = \frac{y^2 - y^4}{\cos\left(\frac{\pi\beta_k}{2}\right)\Gamma(5-\beta_k)}\Big(12(x^{4-\beta_k} + (1-x)^{4-\beta_k} - 6(4-\beta_k)\times$$
$$(x^{3-\beta_k} + (1-x)^{3-\beta_k}) + (3-\beta_k)(4-\beta_k)(x^{2-\beta} + (1-x)^{2-\beta})\Big).$$

The exact solution for the Problem 2 is $v(x,y,t) = t^{1+\alpha_1}(x^2 - x^4)(y^2 - y^4)$, taking $\alpha_1 = 1.8$, $\alpha_2 = 1.5$, $\beta_1 = 1.8$, $\beta_2 = 1.6$ and $\delta\chi = \delta x = \delta y$, the numerical computations are shown in Table 2, while the graphical results are shown in Figure 2.

Table 2. Numerical results of Problem 2.

		L_∞-norm			Convergence					
		$\delta t = 0.1$	$\delta t = 0.01$	$\delta t = 0.001$	$\delta\chi_i$	L_∞	order	δt_i	L_∞	order
	$N = 50$	$8.2070e^{-5}$	$5.9763e^{-5}$	$5.7763e^{-5}$	$\frac{1}{50}$	$5.7763e^{-5}$	—-	0.1	$1.5185e^{-7}$	—-
	$N = 100$	$2.5024e^{-5}$	$1.8192e^{-5}$	$1.7583e^{-5}$	$\frac{1}{100}$	$1.7583e^{-5}$	−0.3531	0.05	$1.2771e^{-7}$	−0.0157
$\theta = 0.5$	$N = 500$	$3.4233e^{-6}$	$2.4844e^{-6}$	$2.4013e^{-6}$	$\frac{1}{500}$	$2.4013e^{-6}$	0.8387	0.01	$1.1017e^{-7}$	−0.0055
	$N = 1000$	$1.8707e^{-6}$	$1.3574e^{-6}$	$1.3120e^{-6}$	$\frac{1}{1000}$	$1.3120e^{-6}$	1.1187	0.005	$1.0810e^{-7}$	−0.0016
	$N = 2000$	$1.5185e^{-7}$	$1.1017e^{-7}$	$1.0648e^{-7}$	$\frac{1}{2000}$	$1.0648e^{-7}$	0.9315	0.001	$1.0648e^{-7}$	−0.0002
	$N = 50$	$7.3450e^{-5}$	$5.9020e^{-5}$	$5.7690e^{-5}$	$\frac{1}{50}$	$5.7690e^{-5}$	—-	0.1	$1.3534e^{-7}$	—-
	$N = 100$	$2.2351e^{-5}$	$1.7964e^{-5}$	$1.7560e^{-5}$	$\frac{1}{100}$	$1.7560e^{-5}$	−0.2885	0.05	$1.2012e^{-7}$	−0.0158
$\theta = 1$	$N = 500$	$1.3663e^{-6}$	$1.0982e^{-6}$	$1.0735e^{-6}$	$\frac{1}{500}$	$1.0735e^{-6}$	0.8521	0.01	$1.0879e^{-7}$	−0.0056
	$N = 1000$	$4.0554e^{-7}$	$3.2597e^{-7}$	$3.1863e^{-7}$	$\frac{1}{1000}$	$3.1863e^{-7}$	1.1199	0.005	$1.0742e^{-7}$	−0.0016
	$N = 2000$	$1.3534e^{-7}$	$1.0879e^{-7}$	$1.0634e^{-7}$	$\frac{1}{2000}$	$1.0634e^{-7}$	−0.9471	0.001	$1.0634e^{-7}$	−0.0004

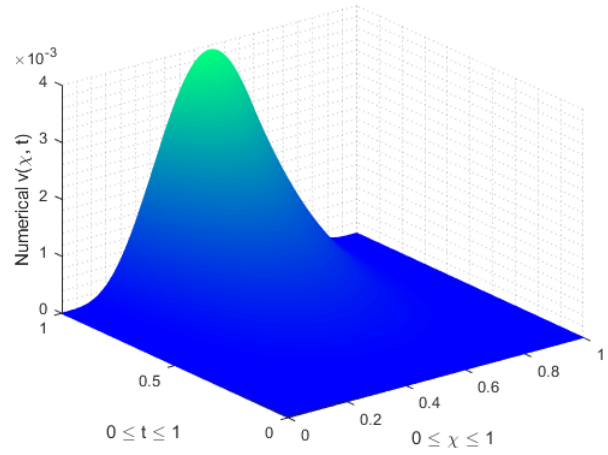

(a) Numerical $v(\chi, t)$ graph

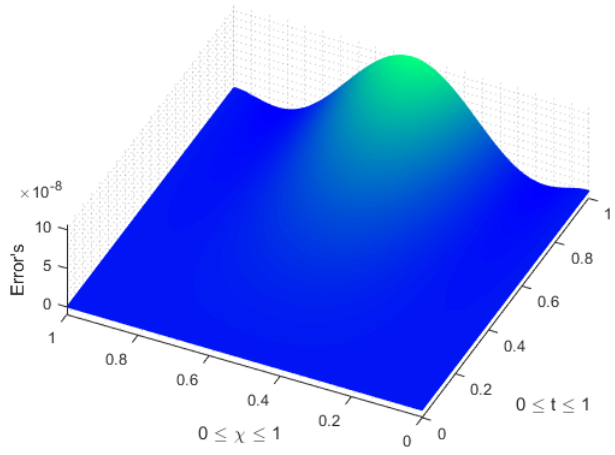

(b) Error graph

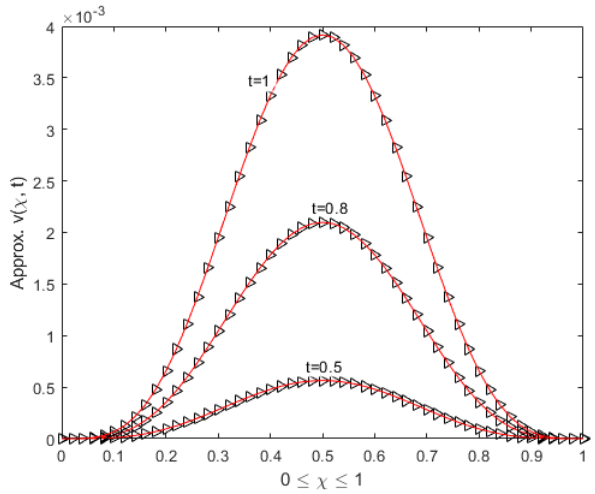

(c) Numerical $v(\chi, t)$

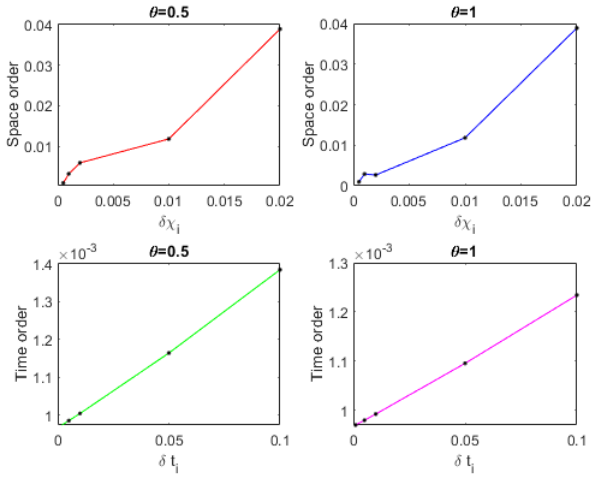

(d) Time and Space convergence graph

Figure 2. Numerical results of Problem 2.

Test Problem 3. Consider the three-dimensional, three term fractional PDE

$$\left({}_0\mathbb{D}_t^{\alpha_1} + {}_0\mathbb{D}_t^{\alpha_2} + {}_0\mathbb{D}_t^{\alpha_3}\right)v(\chi, t) = \sum_{l=1}^{3} \frac{\partial^{\beta_l}}{\partial|\chi|^{\beta_l}} v(\chi, t) + g(\chi, t), \;\; 0 \le \chi \le 1, \;\; t \ge 0,$$

here $0 < \alpha_k \le 1$, $1 < \beta_k \le 2$,

$\chi = (x, y, z)$, Domain $D = [0, 1]^3$ and

$\dfrac{\partial^\beta}{\partial|\chi|^\beta} = \left(\dfrac{\partial^\beta}{\partial|x|^\beta} + \dfrac{\partial^\beta}{\partial|y|^\beta} + \dfrac{\partial^\beta}{\partial|z|^\beta}\right)$ with the following conditions,

$v(\chi, 0) = 0,$

$v(0, t) = 0, \quad v(1, t) = 0,$

$v(x, y, z, t) = t^2(x - x^2)(y - y^2)(z - z^2)$ is the exact solution and

$$g(x, y, z, t) = (x-x^2)(y-y^2)(z-z^2)\sum_{k=1}^{3} \frac{2t^{2-\alpha_k}}{\Gamma(3-\alpha_k)} + t^2\Big[(y-y^2)(z-z^2)h_x + (z-z^2)(x-x^2)h_y + (x-x^2)(y-y^2)h_z\Big]$$

where $h_x = \sum_{k=1}^{3} \frac{1}{-2\cos\left(\frac{\pi\beta_k}{2}\right)}\left(\frac{x^{1-\beta_k}}{\Gamma(2-\beta_k)} - \frac{2x^{2-\beta_k}}{\Gamma(3-\beta_k)}\right)$,

$h_y = \sum_{k=1}^{3} \frac{1}{-2\cos\left(\frac{\pi\beta_k}{2}\right)}\left(\frac{y^{1-\beta_k}}{\Gamma(2-\beta_k)} - \frac{2y^{2-\beta_k}}{\Gamma(3-\beta_k)}\right)$,

$h_z = \sum_{k=1}^{3} \frac{1}{-2\cos\left(\frac{\pi\beta_k}{2}\right)}\left(\frac{z^{1-\beta_k}}{\Gamma(2-\beta_k)} - \frac{2z^{2-\beta_k}}{\Gamma(3-\beta_k)}\right)$,

The numerical results are shown in Table 3, where $\alpha_1 = 0.8, \alpha_2 = 0.5, \alpha_3 = 0.3, \beta_1 = 1.8, \beta_2 = 1.6, \beta_3 = 1.5$ and $\delta\chi = \delta x = \delta y = \delta z$, and the graphical results are shown in Figure 3.

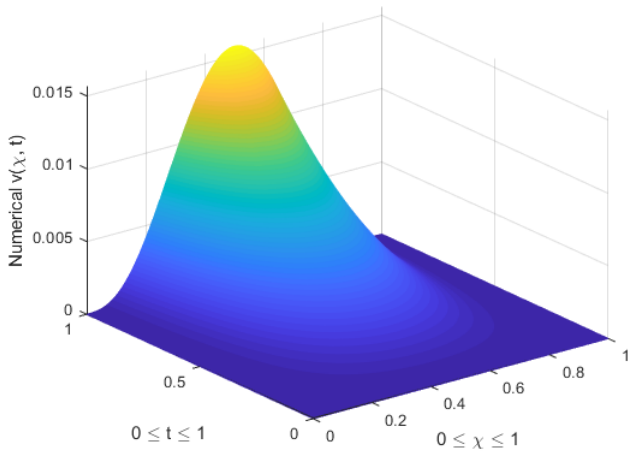

(a) Numerical $v(\chi, t)$ graph

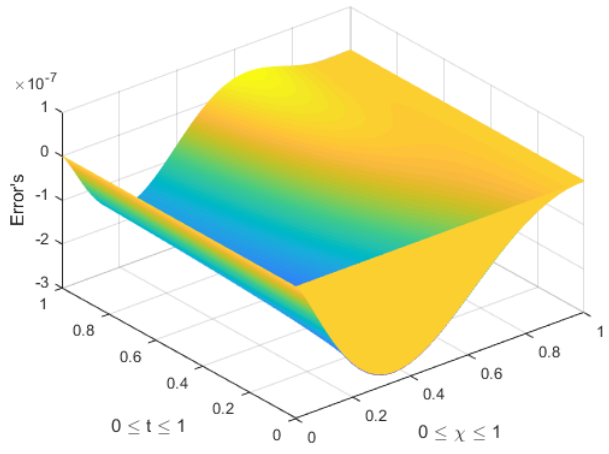

(b) Error graph

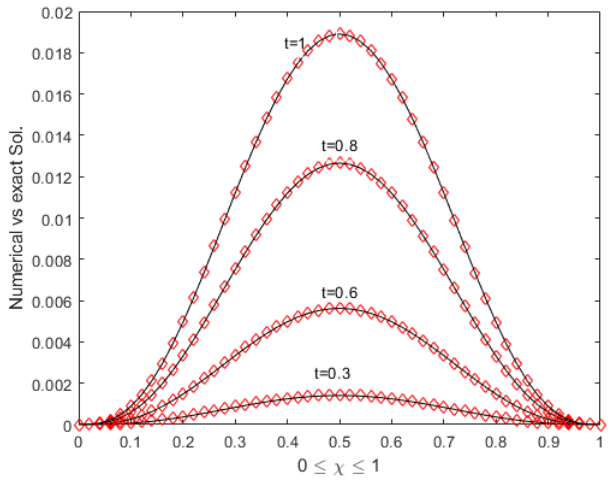

(c) Numerical $v(\chi, t)$

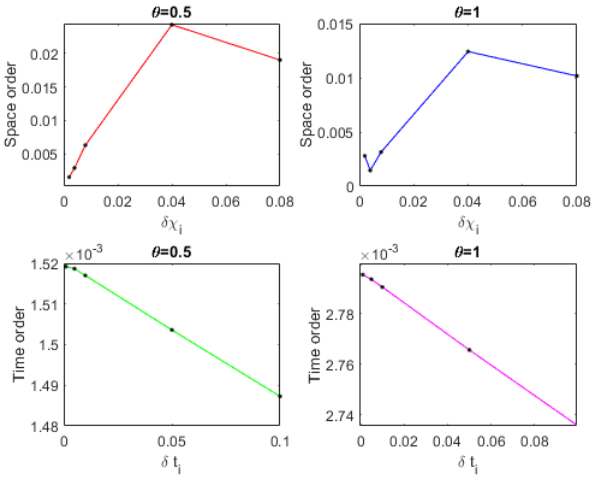

(d) Time and Space convergence graph

Figure 3. Numerical results of Problem 3.

Table 3. Numerical results of Problem 3.

		L_∞-norm			Convergence					
		$\delta t = 0.1$	$\delta t = 0.01$	$\delta t = 0.001$	$\delta\chi_i$	L_∞	order	δt_i	L_∞	order
$\theta = 0.5$	$N = 50$	$3.1498e^{-5}$	$3.1499e^{-5}$	$2.8200e^{-5}$	$\frac{1}{50}$	$2.8200e^{-5}$	—-	0.1	$1.6310e^{-7}$	—-
	$N = 100$	$1.0020e^{-5}$	$1.0148e^{-5}$	$9.7910e^{-6}$	$\frac{1}{100}$	$9.7910e^{-6}$	−0.3531	0.05	$1.6489e^{-7}$	−0.0157
	$N = 500$	$6.7709e^{-7}$	$6.9041e^{-7}$	$6.9002e^{-7}$	$\frac{1}{500}$	$6.9002e^{-7}$	0.8387	0.01	$1.6636e^{-7}$	−0.0055
	$N = 1000$	$3.1128e^{-7}$	$3.1749e^{-7}$	$3.1776e^{-7}$	$\frac{1}{1000}$	$3.1776e^{-7}$	1.1187	0.005	$1.6654e^{-7}$	−0.0016
	$N = 2000$	$1.6310e^{-7}$	$1.6636e^{-7}$	$1.6660e^{-7}$	$\frac{1}{2000}$	$1.6660e^{-7}$	0.9315	0.001	$1.6660e^{-7}$	−0.0002
$\theta = 1$	$N = 50$	$1.5797e^{-5}$	$1.5968e^{-5}$	$1.5089e^{-5}$	$\frac{1}{50}$	$1.5089e^{-5}$	—-	0.1	$8.1549e^{-8}$	—-
	$N = 100$	$5.0150e^{-6}$	$5.0962e^{-6}$	$5.0095e^{-6}$	$\frac{1}{100}$	$5.0095e^{-6}$	−0.2885	0.05	$8.2445e^{-8}$	−0.0158
	$N = 500$	$3.3857e^{-7}$	$3.4531e^{-7}$	$3.4556e^{-7}$	$\frac{1}{500}$	$3.4556e^{-7}$	0.8521	0.01	$8.3187e^{-8}$	−0.0056
	$N = 1000$	$1.5565e^{-7}$	$1.5876e^{-7}$	$1.5900e^{-7}$	$\frac{1}{1000}$	$1.5900e^{-7}$	1.1199	0.005	$8.3278e^{-8}$	−0.0016
	$N = 2000$	$8.1549e^{-8}$	$8.3187e^{-8}$	$8.3332e^{-8}$	$\frac{1}{2000}$	$8.3332e^{-8}$	−0.9471	0.001	$8.3332e^{-8}$	−0.0004

Test Problem 4. Consider the following three-dimensional, three term fractional PDE

$$\left({}_0\mathbb{D}_t^{\alpha_1} + {}_0\mathbb{D}_t^{\alpha_2} + {}_0\mathbb{D}_t^{\alpha_3}\right)v(\chi,t) = \sum_{l=1}^{3} \frac{\partial^{\beta_l}}{\partial|\chi|^{\beta_l}} v(\chi,t) + g(\chi,t), \quad t \geq 0, \quad 0 \leq \chi \leq \frac{\pi}{2},$$

here $\chi = (x,y,z)$ and $\dfrac{\partial^\beta}{\partial|\chi|^\beta} = \left(\dfrac{\partial^\beta}{\partial|x|^\beta} + \dfrac{\partial^\beta}{\partial|y|^\beta} + \dfrac{\partial^\beta}{\partial|z|^\beta}\right)$, Domain $D = [0, \frac{\pi}{2}]^3$ with the following initial and boundary conditions

$v(\chi,0) = 0, \quad v_t(\chi,0) = 0;$

$v(0,t) = 0, \quad v(\frac{\pi}{2},t) = t^2$

$v(x,y,z,t) = t^2 \sin x \sin y \sin z$

$$g(x,y,z,t) = 2\sin x \sin y \sin z \sum_{k=1}^{3} \left(\frac{t^{2-\alpha_k}}{\Gamma(3-\alpha_k)}\right) - t^2\Big(h_x \sin y \sin z + h_y \sin z \sin x + h_z \sin x \sin y\Big),$$

where $h_x = \sum_{k=1}^{3} \dfrac{\sin(x + \frac{\pi}{2}\beta_k)}{2\cos\left(\frac{\pi\beta_k}{2}\right)}$, $h_y = \sum_{k=1}^{3} \dfrac{\sin(y + \frac{\pi}{2}\beta_k)}{2\cos\left(\frac{\pi\beta_k}{2}\right)}$ and $h_z = \sum_{k=1}^{3} \dfrac{\sin(z + \frac{\pi}{2}\beta_k)}{2\cos\left(\frac{\pi\beta_k}{2}\right)}$,

The numerical approximation are shown in Table 4, where $\alpha_1 = 1.4, \alpha_2 = 1.5, \alpha_3 = 1.8, \beta_1 = 1.5$, $\beta_2 = 1.6$, $\beta_3 = 1.8$ and $\delta\chi = \delta x = \delta y = \delta z$ while the graphical results are highlighted in Figure 4.

Table 4. Numerical results of Problem 4.

		L_∞-norm			Convergence					
		$\delta t = 0.1$	$\delta t = 0.01$	$\delta t = 0.001$	$\delta\chi_i$	L_∞	order	δt_i	L_∞	order
$\theta = 0.5$	$N = 50$	$4.7032e^{-4}$	$4.5890e^{-5}$	$4.5813e^{-5}$	$\frac{\pi}{100}$	$4.5813e^{-5}$	—-	0.1	$9.6855e^{-6}$	—-
	$N = 100$	$1.5833e^{-5}$	$1.4792e^{-5}$	$1.4768e^{-5}$	$\frac{\pi}{200}$	$1.4768e^{-5}$	1.6333	0.05	$4.7800e^{-6}$	1.0188
	$N = 500$	$1.3343e^{-5}$	$8.7953e^{-6}$	$4.9924e^{-6}$	$\frac{\pi}{1000}$	$1.7924e^{-6}$	0.5010	0.01	$9.4229e^{-7}$	0.1996
	$N = 1000$	$1.1123e^{-5}$	$3.7645e^{-6}$	$9.7489e^{-7}$	$\frac{\pi}{2000}$	$9.7489e^{-7}$	−1.0007	0.005	$4.7073e^{-7}$	1.0013
	$N = 2000$	$9.6855e^{-6}$	$9.4229e^{-7}$	$9.4078e^{-8}$	$\frac{\pi}{4000}$	$9.4078e^{-8}$	1.4941	0.001	$9.4078e^{-8}$	0.1911
$\theta = 1$	$N = 50$	$2.2231e^{-4}$	$4.5849e^{-5}$	$4.5809e^{-5}$	$\frac{\pi}{100}$	$4.5809e^{-5}$	—-	0.1	$9.4902e^{-6}$	—-
	$N = 100$	$1.5403e^{-5}$	$1.4779e^{-5}$	$1.4767e^{-5}$	$\frac{\pi}{200}$	$1.4767e^{-5}$	1.6333	0.05	$4.7241e^{-6}$	1.0064
	$N = 500$	$3.0656e^{-5}$	$9.9460e^{-6}$	$9.9381e^{-6}$	$\frac{\pi}{1000}$	$9.9381e^{-6}$	−0.5633	0.01	$9.4145e^{-7}$	0.1929
	$N = 1000$	$1.0026e^{-5}$	$3.0412e^{-6}$	$3.0387e^{-7}$	$\frac{\pi}{2000}$	$3.0387e^{-7}$	3.1522	0.005	$4.7052e^{-7}$	1.0006
	$N = 2000$	$9.4902e^{-6}$	$9.4145e^{-7}$	$9.3589e^{-8}$	$\frac{\pi}{4000}$	$9.3589e^{-8}$	−0.1802	0.001	$9.3589e^{-8}$	0.1941

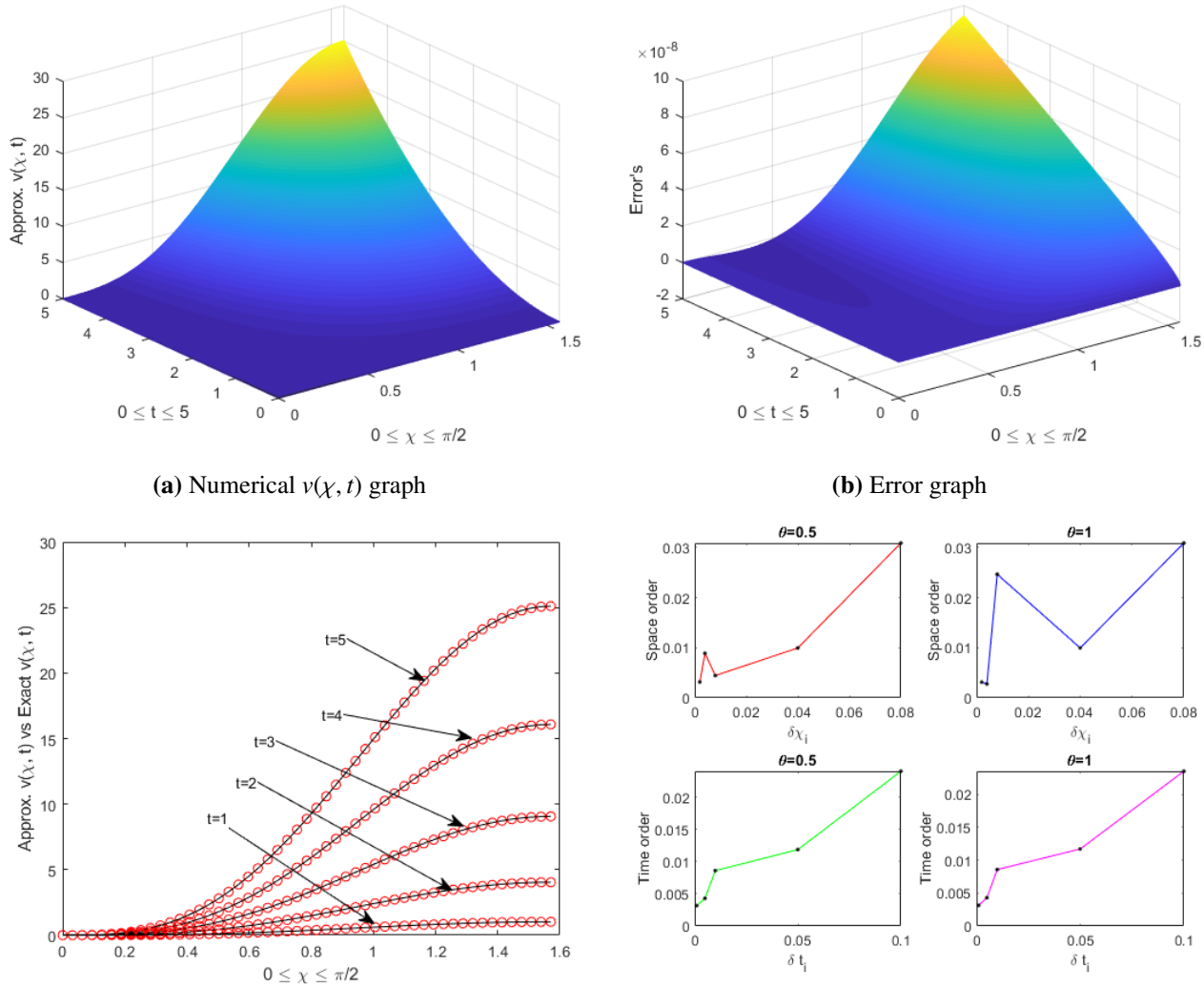

(a) Numerical $v(\chi, t)$ graph

(b) Error graph

(c) Numerical $v(\chi, t)$

(d) Time and Space convergence graph

Figure 4. Numerical results of Problem 4.

6. Conclusions

In this work, meshfree numerical scheme for some multi terms diffusion equations is discussed. The method is tested on some numerical examples. The space derivatives are dealt by Riesz, Rieman-Liouville, Grünwald-Letnikov fractional derivatives while time derivatives are dealt by Caputo fractional derivative method. Further RBF method is used for space discretization, while time iterations are performed by finite difference method. The accuracy of the numerical scheme is assessed by L_∞-norm. The space and time convergence rates for all problems are computed numerically as well as graphically. The stability of the scheme is also discussed after formation of numerical scheme and numerical results confirm that the accuracy increases as the number of collocation points increase.

Conflict of interest

There is no conflict of interest.

References

1. M. Abbaszadeh, M. Dehghan, An improved meshless method for solving two-dimensional distributed order time-fractional diffusion-wave equation with error estimate, *Numer. Algorithms*, **75** (2017), 173–211. https://doi.org/10.1007/s11075-016-0201-0
2. S. Qin, F. Liu, I. Turner, V. Veghc, Q. Yu, Q. Yang, Multi-term time-fractional Bloch equations and application in magnetic resonance imaging, *J. Comput. Appl. Math.*, **319** (2017), 308–319. https://doi.org/10.1016/j.cam.2017.01.018
3. V. Srivastava, K. N. Rai, A multi-term fractional diffusion equation for oxygen delivery through a capillary to tissues, *Math. Comput. Model.*, **51** (2010), 616–624. https://doi.org/10.1016/j.mcm.2009.11.002
4. Y. Zhang, D. A. Benson, D. M. Reeves, Time and space nonlocalities underlying fractional-derivative models: Distinction and literature review of field applications, *Adv. Water Resour.*, **32** (2009), 561–581. https://doi.org/10.1016/j.advwatres.2009.01.008
5. E. Bazhlekova, I. Bazhlekov, Subordination approach to multi-term time-fractional diffusion-wave equations, *J. Comput. Appl. Math.*, **339** (2018), 179–192. https://doi.org/10.1016/j.cam.2017.11.003
6. H. Jiang, F. Liu, I. Turner, K. Burrage, Analytical solutions for the multi-term time-space Caputo-Riesz fractional advection-diffusion equations on a finite domain, *J. Math. Anal. Appl.*, **389** (2012), 1117–1127. https://doi.org/10.1016/j.jmaa.2011.12.055
7. S. Shen, F. Liu, V. Anh, The analytical solution and numerical solutions for a two-dimensional multi-term time fractional diffusion and diffusion-wave equation, *J. Comput. Appl. Math.*, **345** (2019), 515–534. https://doi.org/10.1016/j.cam.2018.05.020
8. Y. Zhao, Y. Zhang, F. Liu, I. Turner, D.Y. Shi, Analytical solution and nonconforming finite element approximation for the 2D multi-term fractional subdiffusion equation, *Appl. Math. Model.*, **40** (2016), 8810–8825. https://doi.org/10.1016/j.apm.2016.05.039
9. X. Tian, S. Y. Reutskiy, Z. J. Fu, A novel meshless collocation solver for solving multi-term variable-order time fractional PDEs, *Eng. Comput.*, 2021, 1–12.
10. M. Cai, C. Li, On Riesz derivative, *Fract. Calc. Appl. Anal.*, **22** (2019), 287–301. https://doi.org/10.1007/s00366-021-01298-7
11. M. Cai, C. Li, *Theory and numerical approximations of fractional integrals and derivatives*, SIAM, 2019. https://doi.org/10.1515/fca-2019-0019
12. H. Ding, C. Li, High-order numerical algorithms for Riesz derivatives via constructing new generating functions, *J. Sci. Comput.*, **71** (2017), 759–784.
13. H. Ding, C. Li, Y. Chen, High-order algorithms for Riesz derivative and their applications (II), *J. Comput. Phys.*, **293** (2015), 218–237. https://doi.org/10.1007/s10915-016-0317-3

14. M. M. A. Khater, S. K. Elagan, M. A. El-Shorbagy, S. H. Alfalqi, J. F. Alzaidi, N. A. Alshehri, Folded novel accurate analytical and semi-analytical solutions of a generalized Calogero-Bogoyavlenskii-Schiff equation, *Commun. Theor. Phys.*, **73** (2021), 095003.

15. M. M. A. Khater, D. Lu, Analytical versus numerical solutions of the nonlinear fractional time-space telegraph equation, *Mod. Phys. Lett. B*, **35** (2021) 2150324. https://doi.org/10.1088/1572-9494/ac049f

16. R. A. M. Attia, J. Tian, D. Lu, J. F. G. Aguilar, M. M. A. Khater, Unstable novel and accurate soliton wave solutions of the nonlinear biological population model, *Arab J. Basic Appl. Sci.*, **29** (2022), 19–25. https://doi.org/10.1142/S0217984921503243 https://doi.org/10.1080/25765299.2021.2024652

17. V. Daftardar-Gejji, S. Bhalekar, Solving multi-term linear and non-linear diffusion-wave equations of fractional order by Adomian decomposition method, *Appl. Math. Comput.*, **202** (2008), 113–120. https://doi.org/10.1016/j.amc.2008.01.027

18. M. A. Jafari, A. Aminataei, An algorithm for solving multi-term diffusion-wave equations of fractional order, *Comput. Math. Appl.*, **62** (2011), 1091–1097. https://doi.org/10.1016/j.camwa.2011.03.066

19. F. Liu, M. M. Meerschaert, R. J. McGough, P. Zhuang, Q. Liu, Numerical methods for solving the multi-term time-fractional wave-diffusion equation, *Fract. Calc. Appl. Anal.*, **16** (2013), 9–25. https://doi.org/10.2478/s13540-013-0002-2

20. A. H. Bhrawy, M. A. Zaky, A method based on the Jacobi tau approximation for solving multi-term time-space fractional partial differential equations, *J. Comput. Phys.*, **281** (2015), 876–895. https://doi.org/10.1016/j.jcp.2014.10.060

21. J. Ren, Z. Z. Sun, Efficient numerical solution of the multi-term time fractional diffusion-wave equation, *East Asian J. Appl. Math.*, **5** (2015), 1–28. https://doi.org/10.4208/eajam.080714.031114a

22. M. Dehghan, M. Safarpoor, M. Abbaszadeh, Two high-order numerical algorithms for solving the multi-term time fractional diffusion-wave equations, *J. Comput. Appl. Math.*, **290** (2015), 174–195. https://doi.org/10.1016/j.cam.2015.04.037

23. M. Abbaszadeh, Error estimate of second-order finite difference scheme for solving the Riesz space distributed-order diffusion equation, *Appl. Math. Lett.*, **88** (2019), 179–185. https://doi.org/10.1016/j.aml.2018.08.024

24. M. Abbaszadeh, M. Dehghan, Numerical and analytical investigations for neutral delay fractional damped diffusion-wave equation based on the stabilized interpolating element free Galerkin (IEFG) method, *Appl. Numer. Math.*, **145** (2019), 488–506. https://doi.org/10.1016/j.apnum.2019.05.005

25. M. Dehghan, M. Abbaszadeh, Spectral element technique for nonlinear fractional evolution equation, stability and convergence analysis, *Appl. Numer. Math.*, **119** (2017), 51–66.

26. M. Dehghan, M. Abbaszadeh, An efficient technique based on finite difference/finite element method for solution of two-dimensional space/multi-time fractional Bloch-Torrey equations, *Appl. Numer. Math.*, **131** (2018), 190–206. https://doi.org/10.1016/j.apnum.2018.04.009

27. H. Chen, S. Lü, W. Chen, A unified numerical scheme for the multi-term time fractional diffusion and diffusion-wave equations with variable coefficients, *J. Comput. Appl. Math.*, **330** (2018), 380–397. https://doi.org/10.1016/j.cam.2017.09.011

28. F. Safari, W. Chen, Coupling of the improved singular boundary method and dual reciprocity method for multi-term time-fractional mixed diffusion wave equations, *Comput. Math. Appl.*, **78** (2019), 1594–1607. https://doi.org/10.1016/j.camwa.2019.02.001

29. J. Huang, J. Zhang, S. Arshad, Y. Tang, A numerical method for two-dimensional multi-term time-space fractional nonlinear diffusion-wave equations, *Appl. Nume. Math.*, **159** (2021), 159–173. https://doi.org/10.1016/j.apnum.2020.09.003

30. Z. J. Fu, S. Reutskiy, H. G. Sun, J. Ma, M. A. Khan, A robust kernel-based solver for variable-order time fractional PDEs under 2D/3D irregular domains, *Appl. Math. Lett.*, **94** (2019), 105–111.

31. Q. Xi, Z. J. Fu, T. Rabczuk, D. Yin, A localized collocation scheme with fundamental solutions for long-time anomalous heat conduction analysis in functionally graded materials, *Int. J. Heat Mass Tran.*, **180** (2021), 121778. https://doi.org/10.1016/j.ijheatmasstransfer.2021.121778

32. H. Wendland, *Approximation scattered data*, Press Cambridge University, Cambridge, 2005.

33. P. Thounthong, M. N. Khan, I. Hussain, I. Ahmad, P. Kumam, Symmetric radial basis function method for simulation of elliptic partial differential equations, *Mathematics*, **6** (2018), 327. https://doi.org/10.3390/math6120327

34. C. C. Piret, E. Hanert, A radial basis functions method for fractional diffusion equations, *J. Comput. Phys.*, **238** (2013), 71–81. https://doi.org/10.1016/j.jcp.2012.10.041

35. V. R. Hosseini, W. Chen, Z. Avazzadeh, Numerical solution of fractional telegraph equation by using radial basis functions, *Eng. Anal. Boundary Elem.*, **38** (2014), 31–39. https://doi.org/10.1016/j.enganabound.2013.10.009

36. I. Ahmad, Mehnaz, S. Islam, S. Zaman, Local meshless differential quadrature collocation method for time-fractional PDEs, *Discrete Cont. Dyn.-S*, 2018. https://doi.org/10.3934/dcdss.2020223

37. A. Samad, J. Muhammad, Meshfree collocation method for higher order KdV equations, *J. Appl. Comput. Mech.*, **7** (2021), 422–431.

38. S. Islam, S. Haq, A. Ali, A meshfree method for the numerical solution of the RLW equation, *J. Comput. Appl. Math.*, **223** (2009), 997–1012.

39. Q. Shen, Local RBF-based differential quadrature collocation method for the boundary layer problems, *Eng. Anal. Boundary Elem.*, **34** (2010), 213–228. https://doi.org/10.1016/j.enganabound.2009.10.004

40. S. Islam, I. Ahmad, A comparative analysis of local meshless formulation for multi-asset option models, *Eng. Anal. Boundary Elem.*, **65** (2016), 159–176.

41. P. Thounthong, M. N. Khan, I. Hussain, I. Ahmad, P. Kumam, Symmetric radial basis function method for simulation of elliptic partial differential equations, *Mathematics*, **6** (2018), 327. https://doi.org/10.3390/math6120327

42. S. Wei, W. Chen, Y. C. Hon, Implicit local radial basis function method for solving two-dimensional time fractional diffusion equations, *Therm. Sci.*, **19** (2015), S59–S67,. https://doi.org/10.2298/TSCI15S1S59W

43. G. E. Fasshauer, *Meshfree approximation methods with matlab*, Word Scientific Publishing Co. Pte. Ltd, 2007.

44. G. Jumarie, Stock exchange fractional dynamics defined as fractional exponential growth driven by (usual) Gaussian white noise. Application to fractional Black-Scholes equations, *Insur. Math. Econ.*, **42** (2008), 271–287. https://doi.org/10.1016/j.insmatheco.2007.03.001

45. G. Jumarie, Derivation and solutions of some fractional Black-Scholes equations in coarse-grained space and time. Application to merton's optimal portfolio, *Comput. Math. Appl.*, **59** (2010), 1142–1164.

46. M. Caputo, Linear models of dissipation whose Q is almost frequency independent-II, *Geophys. J. Int.*, **13** (1967), 529–539. https://doi.org/10.1111/j.1365-246X.1967.tb02303.x

47. Q. Yang, F. Liu, I. Turner, Numerical methods for fractional partial differential equations with Riesz space fractional derivatives, *Appl. Math. Model.*, **34** (2010), 200–218. https://doi.org/10.1016/j.apm.2009.04.006

48. Z. Z. Sun, X. Wu, A fully discrete difference scheme for a diffusion-wave system, *Appl. Numer. Math.*, **56** (2006), 193–209. https://doi.org/10.1016/j.apnum.2005.03.003

49. H. Jalalinejad, A. Tavakoli, F. Zarmehi, A simple and flexible modification of Grünwald-Letnikov fractional derivative in image processing, *Math. Sci.*, **12** (2018), 205–210. https://doi.org/10.1007/s40096-018-0260-6

50. S. Shen, F. Liu, V. Anh, Numerical approximations and solution techniques for the space-time Riesz-Caputo fractional advection-diffusion equation, *Numer. Algorithms*, **56** (2011), 383–403.

AIMS Press